



**ORIGINAL ARTICLE**

# Extracellular ATP promotes breast cancer invasion and epithelial-mesenchymal transition via hypoxia-inducible factor 2 $\alpha$ signaling

Hui Yang<sup>1,2</sup> | Yue-Hang Geng<sup>1</sup> | Peng Wang<sup>3</sup> | Yan-Ting Zhou<sup>1,2</sup> | Han Yang<sup>1,2</sup> | Yan-Fei Huo<sup>1,2</sup> | Hong-Quan Zhang<sup>3</sup>  | Yan Li<sup>1</sup> | Hui-Ying He<sup>1,2</sup> | Xin-Xia Tian<sup>1,2</sup>  | Wei-Gang Fang<sup>1,2</sup>

<sup>1</sup>Department of Pathology, Key Laboratory of Carcinogenesis and Translational Research (Ministry of Education), School of Basic Medical Sciences, Peking University Health Science Center, Beijing, China

<sup>2</sup>Department of Pathology, Peking University Third Hospital, Beijing, China

<sup>3</sup>Department of Anatomy, Histology and Embryology, Peking University Health Science Center, Beijing, China

**Correspondence**

Xin-Xia Tian and Wei-Gang Fang,  
Department of Pathology, Peking University Health Science Center, Beijing 100191, China.

Emails: tianxinxia@bjmu.edu.cn; wgfang@bjmu.edu.cn

**Funding information**

National Natural Science Foundation of China, Grant/Award Number: 81621063 and 81872382

**Abstract**

Extracellular ATP has been shown to play an important role in invasion and the epithelial-mesenchymal transition (EMT) process in breast cancer; however, the mechanism is unclear. Here, by using a cDNA microarray, we demonstrated that extracellular ATP could stimulate hypoxia-inducible factor (HIF) signaling and up-regulate hypoxia-inducible factor 1/2 $\alpha$  (HIF-1/2 $\alpha$ ) expression. After knocking down HIF-1/2 $\alpha$  using siRNA, we found that ATP-driven invasion and EMT were significantly attenuated via HIF2A-siRNA in breast cancer cells. By using ChIP assays, we revealed that the biological function of extracellular ATP in invasion and EMT process depended on HIF-2 $\alpha$  direct targets, among which lysyl oxidase-like 2 (LOXL2) and matrix metalloproteinase-9 (MMP-9) mediated ATP-driven invasion, and E-cadherin and Snail mediated ATP-driven EMT, respectively. In addition, using silver staining and mass spectrometry, we found that phosphoglycerate kinase 1 (PGK1) could interact with HIF-2 $\alpha$  and mediate ATP-driven HIF-2 $\alpha$  upregulation. Furthermore, we demonstrated that expressions of HIF-2 $\alpha$  and its target proteins could be regulated via ATP by AKT-PGK1 pathway. Using a Balb/c mice model, we illustrated the function of HIF-2 $\alpha$  in promoting tumor growth and metastasis *in vivo*. Moreover, by exploring online databases, we found that molecules involved in ATP-HIF-2 $\alpha$  signaling were highly expressed in human breast carcinoma tissues and were associated with poor prognosis. Altogether, these findings suggest that extracellular ATP could promote breast carcinoma invasion and EMT via HIF-2 $\alpha$  signaling, which may be a potential target for future anti-metastasis therapy.

**KEYWORDS**

breast cancer, epithelial-mesenchymal transition, extracellular ATP, HIF-2 $\alpha$ , invasion

## 1 | INTRODUCTION

ATP, which has been considered as an energy source,<sup>1</sup> is also involved in the determination of cell fate,<sup>2</sup> proliferation,<sup>3</sup> metabolism,<sup>4</sup> differentiation<sup>5</sup> and apoptosis.<sup>3</sup> Thereby, it is possible that ATP plays a vital role in promoting or preventing malignant transformation. The amount of extracellular ATP is negligible in healthy tissues.<sup>6,7</sup> By contrast, ATP accumulates at high levels in tumor sites,<sup>8,9</sup> reaching hundreds of micromoles in the host-tumor interface.<sup>9,10</sup> The pro-invasive activity of ATP was first described in Fang et al.<sup>11</sup> However, the mechanism in breast cancer has not yet been resolved. Our previous studies have demonstrated that extracellular ATP is vital for cancer cell invasion and epithelial-mesenchymal transition (EMT) through activating P2Y2 and/or P2X7 to regulate the expressions of associated molecules, including IL-8, Snail, Claudin-1, E-cadherin,  $\beta$ -catenin and S100A4, as well as via activation of EGFR and ERK1/2.<sup>1,11-16</sup>

Endothelial PAS domain protein 1 (EPAS1) is a member of a basic-helix-loop-helix/PAS domain containing transcription factors, which has a high homology to hypoxia-inducible factor 1 $\alpha$  (HIF-1 $\alpha$ ); thus, it is also termed hypoxia-inducible factor 2 $\alpha$  (HIF-2 $\alpha$ ).<sup>17</sup> Like HIF-1 $\alpha$ , HIF-2 $\alpha$  could function by forming a complex with aryl hydrocarbon receptor nuclear translocator (ARNT; also termed HIF-1 $\beta$ ) and transactivates target genes to respond to environmental stressors such as hypoxia.<sup>18</sup> In addition, HIF-2 $\alpha$  could transactivate genes, particularly those involved in angiogenesis, anaerobic metabolism, invasion and anti-apoptosis.<sup>19,20</sup> Although the dominant role of HIF-1 $\alpha$  in controlling responses to hypoxia and tumorigenesis is well established, the vital function of HIF-2 $\alpha$  in cancer is a relatively new topic.<sup>21</sup> Some evidence suggests that HIF-2 $\alpha$  drives tumor progression in renal cell carcinomas (RCC) in which there is a gradual shift from HIF-1 $\alpha$  to HIF-2 $\alpha$  expression with increasing tumor grade.<sup>22</sup> Cho et al.<sup>23</sup> demonstrated a significant efficacy of a HIF-2 $\alpha$  antagonist in preclinical kidney cancer models. Moreover, elevated HIF-2 $\alpha$  has been shown to be associated with poor patient prognosis in some tumors such as RCC, astrocytoma, neuroblastoma and glioblastoma<sup>21,24-26</sup>.

Metastasis is a complex multistep process that involves the early steps of tumor EMT and invasion and the late step of metastatic colonization in distant organs.<sup>27</sup> To identify the genes involved in EMT and the invasion process of extracellular ATP, we performed cDNA microarray analysis on MCF-7 cells. We found that mRNA levels of HIF2A and HIF target genes were upregulated via ATP treatment. Hence, we hypothesized that extracellular ATP could drive the metastasis process by upregulating HIF even under normoxic conditions and investigated the mechanism involved.

## 2 | MATERIALS AND METHODS

### 2.1 | Antibodies and reagents

The antibodies were purchased from the following companies. HIF-2 $\alpha$  (ab199), HIF-1 $\alpha$  (ab1), phospho-AKT (T308) (ab38449),

AKT (ab18785), LOXL2 (ab96233) and MMP-9 (ab38898) were from Abcam (Cambridge, UK). PGK1 (NBP2-67534) was from Novus (Cambridge, UK).  $\beta$ -Actin, P2Y2, E-cadherin and Snail were from Santa Cruz Biotechnology (Santa Cruz, CA, USA). HRP-conjugated goat anti-mouse IgG (#ZB-2305), HRP-conjugated goat anti-rabbit IgG (#ZB-2301) were bought from OriGene (Rockville, MD, USA).

The reagents were purchased from the following companies. ATP was bought from Sigma (St Louis, MO, USA). Scrambled control siRNA and siRNAs against HIF1A, HIF2A, AKT, PGK1, LOXL2, MMP9 and P2Y2, were obtained from Shanghai GenePharma Co., Ltd. (Shanghai, China). Protein A/G beads were purchased from Amersham Biosciences (Piscataway, NJ, USA) and protease inhibitor cocktail was bought from Roche Applied Science (Indianapolis, IN, USA). LOXL2 and MMP-9 ELISA Kits were obtained from Abcam. LY294002 (AKT inhibitor) was bought from Selleck (Houston, TX, USA).

### 2.2 | Cell lines and cell culture

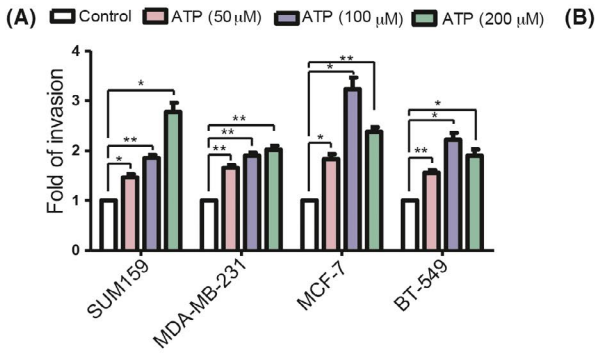
Human breast cancer cell lines MDA-MB-231, BT-549 and normal breast cell line MCF10A were obtained from American Type Culture Collection (ATCC, Manassas, VA, USA). MCF-7 cells were purchased from the Cell Resource Center, Institute of Basic Medical Sciences, Chinese Academy of Medical Sciences (Beijing, China). SUM159 cells were bought from Asterand (Detroit, MI, USA). The culture medium is described in Appendix S1. Cell lines were validated for authentication using the short tandem repeat method. Cells were cultured at 37°C in a humidified CO<sub>2</sub> incubator (5% CO<sub>2</sub>, 95% air). Hypoxic incubations were performed using the InVivo2 Hypoxia Workstation (Biotrace International).

### 2.3 | cDNA microarray and data analyses

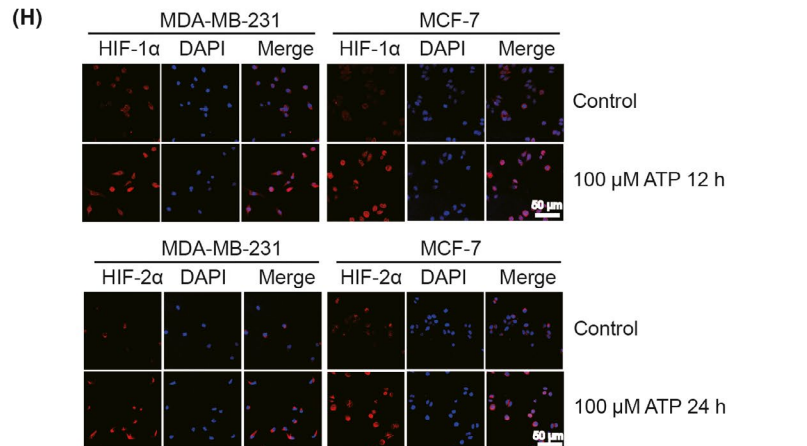
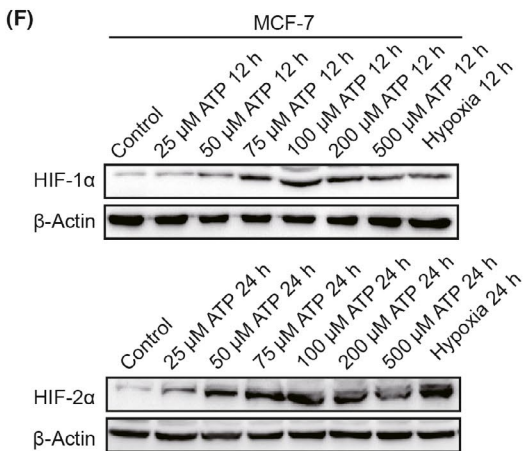
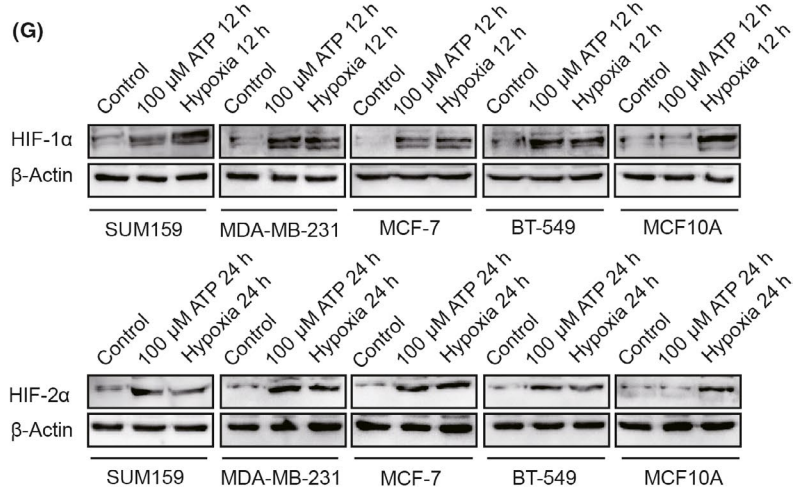
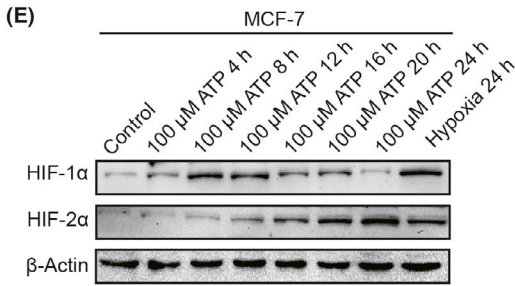
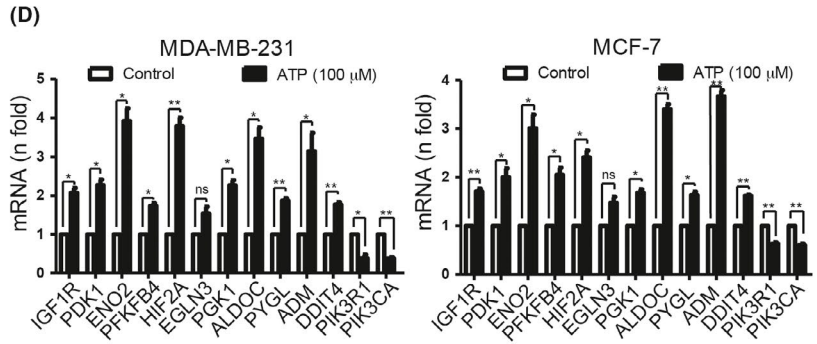
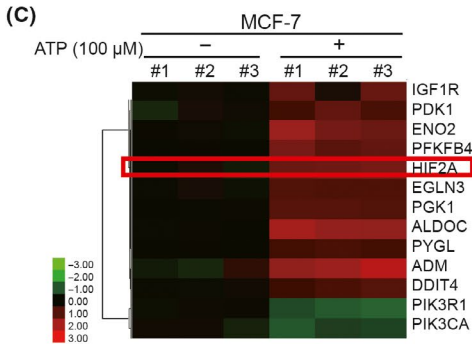
MCF-7 cells were treated with/without 100  $\mu$ mol/L ATP for 24 hours. Total RNA was extracted using Trizol Reagent (Invitrogen, Carlsbad, CA, USA). And then cDNA microarray was performed using Affymetrix Human Genome U133 Plus 2.0 Array (Affymetrix, Santa Clara, CA, USA), which contains 47 000 transcripts and 38 500 clear human genes as described by Zhang et al.<sup>15</sup> Data were analyzed using Student's *t* test, and differently expressed genes in mRNA levels between ATP treatment and control (*n* = 3, each) were determined with a threshold cutoff of 2-fold (*P* < 0.05) in this research (accession number: GSE113757).

### 2.4 | Cell transfection

For transient gene silencing, a scramble siRNA used as a negative control and two distinct siRNA oligonucleotides targeting HIF1A, HIF2A, PGK1, AKT and P2Y2, respectively, were used. Their sequences are shown in Appendix S2. Cells were transfected with indicated siRNA using Lipofectamine RNAi Max (Invitrogen) according to the manufacturer's instructions.



Category	Term	P Value
KEGG PATHWAY	Alcoholism	0.00
KEGG PATHWAY	Glioma	0.01
KEGG PATHWAY	Proteoglycans in cancer	0.01
KEGG PATHWAY	Systemic lupus erythematosus	0.02
KEGG PATHWAY	Amoebiasis	0.02
KEGG PATHWAY	Ovarian steroidogenesis	0.03
KEGG PATHWAY	Transcriptional misregulation in cancer	0.03
KEGG PATHWAY	Glycosphingolipid biosynthesis - ganglio series	0.03
KEGG PATHWAY	FoxO signaling pathway	0.04
KEGG PATHWAY	Small cell lung cancer	0.04
KEGG PATHWAY	Viral carcinogenesis	0.04
KEGG PATHWAY	Prolactin signaling pathway	0.04
KEGG PATHWAY	Chemokine signaling pathway	0.05
KEGG PATHWAY	HIF signaling pathway	0.05
KEGG PATHWAY	Pathways in cancer	0.05



For gene overexpression, cells were transfected with Flag plasmid or Flag-HIF plasmid using Lipofectamine 2000 (Invitrogen) and the stably transfected cells were selected by 500  $\mu\text{g}/\text{mL}$  G418 (Gibco-BRL) for 21 days. See Appendix S3 for plasmid construction.

## 2.5 | In vitro cellular invasion and migration assays

Transwell chamber filters coated with 50  $\mu\text{L}$  Matrigel (BD Biosciences) were prepared for invasion assay and no Matrigel-coated Transwell chamber filters were used for migration assay. Cells were added to the top of chambers in a serum-free DMEM/RPMI 1640. DMEM/RPMI 1640 containing 30% FBS was used in the lower chambers. Cells migrated to the lower surface were fixed in 4% formaldehyde and stained using crystal violet. Seven random fields were counted for each membrane at 200 $\times$  magnification under the microscope.

## 2.6 | Quantitative real-time PCR

Real-time PCR was performed as described by Zhang et al.<sup>15</sup> The primer sequences for quantitative RT-PCR analysis are listed in Appendix S4. Gene expression levels were normalized to  $\beta$ -Actin. The relative expression level of mRNA was evaluated by using the  $2^{-\Delta\Delta\text{CT}}$  method.

## 2.7 | ELISA

Supernatant was collected by centrifuging at 1000  $g$  (for mouse blood) or 10 000  $g$  (for cell culture medium) for 10 minutes at 4 $^{\circ}\text{C}$ . Protein levels of LOXL2 and MMP-9 were measured, respectively, using the LOXL2 and MMP-9 ELISA Kit (Abcam) following the manufacturer's instructions. Protein concentrations were determined by absorbance comparison to the standard curve.

## 2.8 | Immunofluorescence analysis

Experiments were performed as described by Liu<sup>1</sup>, with some modifications. Briefly, cells were incubated with anti-HIF-2 $\alpha$  (1:200) or anti-PGK1 (1:200) antibody at 4 $^{\circ}\text{C}$  overnight, followed by incubation with FITC-conjugated or Texas Red-conjugated IgG fluorescence secondary antibody (1:500 dilution; GIBCO). Finally, the cell nucleus was stained with DAPI (Vector Laboratories, Burlingame, CA, USA) and observed under a confocal microscope (TCS SP2 AOBS, Leica).

## 2.9 | Co-immunoprecipitation analysis

Co-immunoprecipitation was carried out as described by Shan et al.<sup>28</sup> In our research, primary antibody HIF-2 $\alpha$  (1:200, 5  $\mu\text{L}$ ) or PGK1 (1:200, 5  $\mu\text{L}$ ) was used.

## 2.10 | Silver staining and mass spectrometry

Silver staining and mass spectrometry assays were carried out as described by Shan et al.<sup>28</sup> using resultant materials from co-immunoprecipitation analysis. PGK1 enrichment from mass spectrometry is listed in Appendix S5.

## 2.11 | ChIP and quantitative PCR

ChIP experiments were performed as described by Shan et al.<sup>28</sup> Primer sequences used in the qPCR analysis are listed in Appendix S6.

## 2.12 | Western blotting analysis

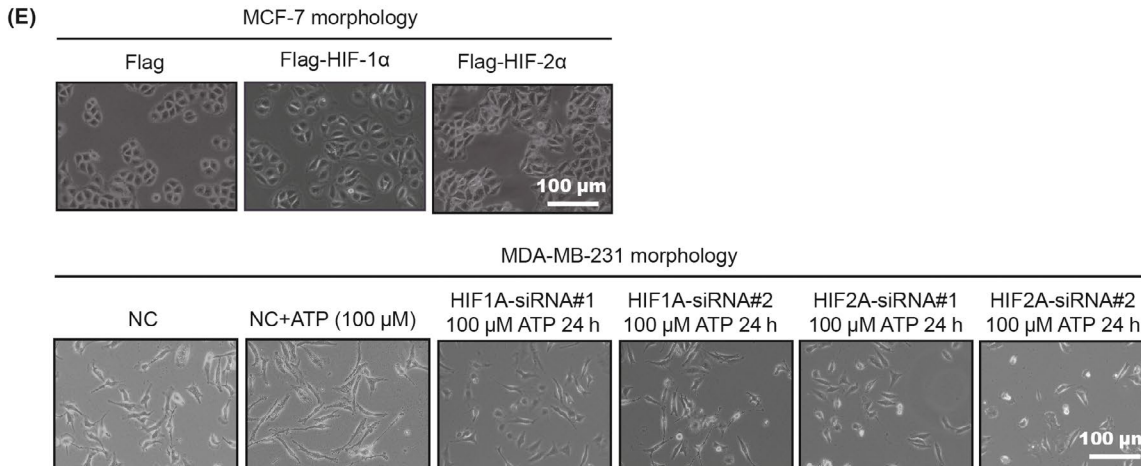
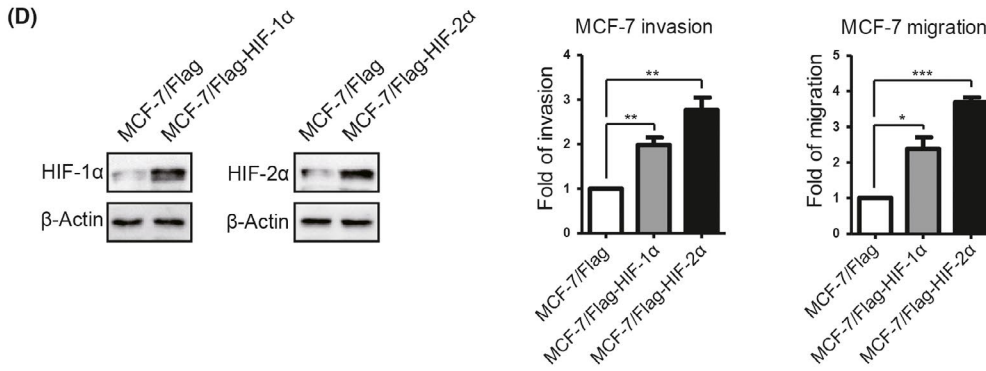
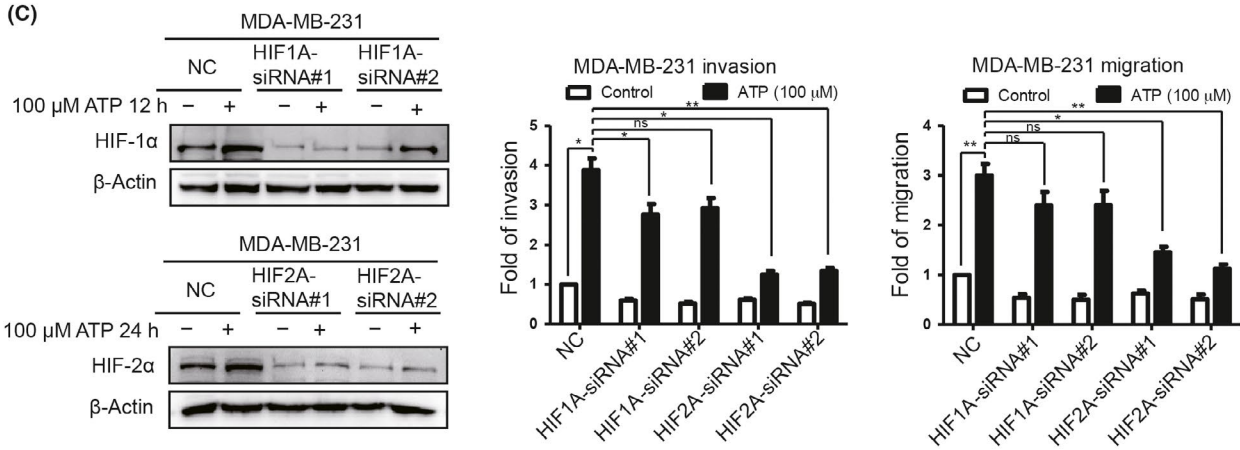
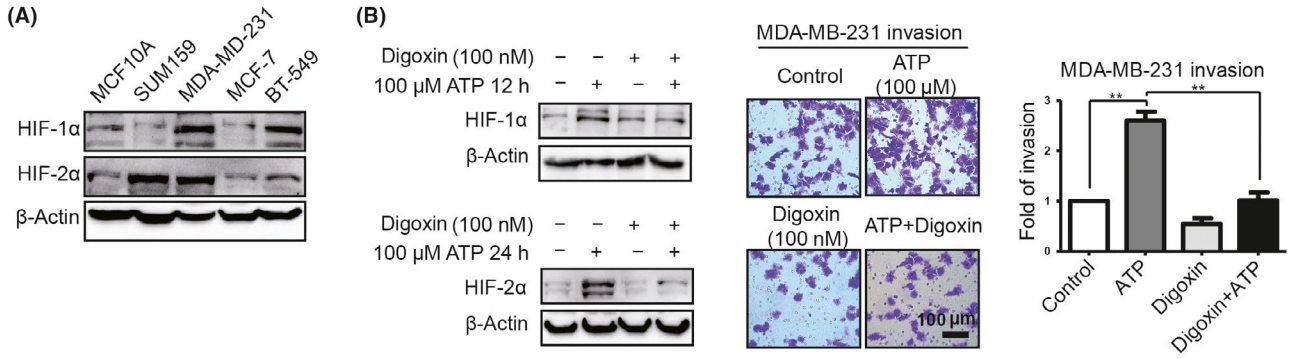
Western blotting analysis were performed as described by Zhang et al.<sup>15</sup> Primary antibodies used: anti-HIF-1 $\alpha$  (1:1000), anti-HIF-2 $\alpha$  (1:1000), anti-PGK1 (1:1000), anti-phospho-AKT (T308) (1:1000), anti-AKT (1:1000), anti-LOXL2 (1:1000), anti-MMP9 (1:1000), anti-E-cadherin (1:500), anti-Snail (1:500), anti-P2Y2 (1:500), and anti- $\beta$ -Actin (1:1000).

Results were presented as the ratio of targeted proteins to  $\beta$ -Actin. Immunoreactive protein was visualized via chemiluminescence (Applygen Technologies Inc., Beijing, China) and quantified via densitometry analysis, using ImageJ software (NIH Image, Bethesda, MD, USA). Uncropped bands are presented in Appendix S7.

## 2.13 | Xenograft tumorigenesis assays

Female Balb/c nude mice of 6 weeks were bred in specific pathogen-free condition at the Center of Experimental Animals (Peking University, Beijing, China). Experimental procedures for using laboratory animals were approved by the Institutional Animal Care and Use Committee of Peking University (No. LA2014229). Five million MCF-7 cells, stably transfected with Flag or Flag-HIF-2 $\alpha$  plasmid, were inoculated into mammary fat pads of mice ( $n = 7$  each group, randomly). Tumor volumes were measured every 2 days. One month after inoculation, mice were killed and primary tumors were collected for quantitative RT-PCR, western blotting, H&E staining and

**FIGURE 1** Extracellular ATP regulates hypoxia-inducible factor (HIF) signaling in breast cancer cells. A, Transwell invasion assays demonstrated that ATP enhanced invasion ability of breast cancer cells. B, MCF-7 cells treated with/without 100  $\mu\text{mol}/\text{L}$  ATP for 24 h were analyzed by cDNA microarray. KEGG pathway analysis showed that ATP significantly affected HIF signaling. C, Heatmaps showed alterations of HIF signaling-related genes. D, Quantitative PCR demonstrated that most HIF signaling-associated genes were upregulated via 24 h ATP treatment. E-G, Western blotting illustrated alterations of HIF-1/2 $\alpha$  in different hours of ATP treatment (E), different concentrations of ATP treatment (F) and in different cells (G). H, Immunofluorescence showed that ATP increased HIF-1/2 $\alpha$  level. Error bars represent means  $\pm$  SD from triplicates. \* $P < 0.05$ ; \*\* $P < 0.01$ ; ns, not significant



immunohistochemistry (IHC) assays. Peripheral blood was collected for ELISA assay. Organs including lungs, livers, kidneys, spleens and hearts were collected for H&E staining. The study was performed in accordance with the Declaration of Helsinki.

### 2.14 | H&E staining and immunohistochemical staining

For histological examination, 4- $\mu$ m sections were stained with H&E and IHC using standard protocol. Primary antibodies used: anti-HIF-2 $\alpha$  (1:100), anti-LOXL2 (1:100), anti-MMP-9 (1:200), anti-E-cadherin (1:200) and anti-Snail (1:200). Data were collected from an average of 10 randomly selected areas for each section by using Image Pro-Plus (IPP) (Media Cybernetics, Silver Spring, MD, USA).

### 2.15 | Data analysis and statistics

All experiments were repeated at least in triplicate. Data are shown as means  $\pm$  SD. The data were analyzed with SPSS 20.0. Student's *t* test was used to determine whether there was a significant difference between 2 groups. Nonparametric ANOVA was performed when multiple means were compared. Statistical significance was considered when  $P \leq 0.05$ .

## 3 | RESULTS

### 3.1 | Extracellular ATP regulates hypoxia-inducible factor signaling in breast cancer cells

We demonstrated that 100  $\mu$ mol/L extracellular ATP treatment led to maximal invasion capacity in breast cancer cells<sup>1,15</sup> (Figure 1A). To identify the molecular mechanism involved, we treated MCF-7 with/without 100  $\mu$ mol/L ATP for 24 hours and performed cDNA microarray analysis (Accession: GSE113757). KEGG pathway analysis of the cDNA microarray data showed that ATP could significantly regulate HIF signaling (Figure 1B), including HIF2A and HIF target genes, such as PDK1 and ENO2<sup>29</sup> (Figure 1C).

To prove this finding, we examined HIF signaling-associated genes by quantitative RT-PCR. Most HIF target genes exhibited increased mRNA levels after ATP treatment in MDA-MB-231 and MCF-7 (Figure 1D). In addition, we detected HIF-1/2 $\alpha$  alterations after different hours (Figure 1E) and concentrations (Figure 1F) of ATP treatment in breast cancer cells and human mammary epithelial cells, MCF10A (Figure 1G). Here, hypoxia was used as a positive

control. As a result, 100  $\mu$ mol/L ATP significantly increased HIF-1/2 $\alpha$  expression in breast cancer cells. The elevation of HIF-1/2 $\alpha$  was also demonstrated via immunofluorescence (Figure 1H).

### 3.2 | Hypoxia-inducible factor-2 $\alpha$ mediates ATP-promoted invasion and epithelial-mesenchymal transition in vitro

To investigate whether HIF could promote invasion and EMT of breast cancer cells in vitro, we first measured HIF-1/2 $\alpha$  levels in different cells. Triple-negative breast cancer cells MDA-MB-231 exhibited higher expression of HIF-1/2 $\alpha$  than MCF10A, while the HIF-1/2 $\alpha$  level in MCF-7 was relatively lower (Figure 2A). Therefore, we used digoxin (100 nmol/L), a well-known inhibitor of HIF,<sup>30</sup> to inhibit HIF-1/2 $\alpha$  expression in MDA-MB-231. As a result, ATP-promoted invasion was attenuated by digoxin (Figure 2B). To determine which HIF played a dominant role in this process, we introduced 2 siRNA against HIF1A and HIF2A, respectively. As a result, HIF2A-siRNA significantly decreased ATP-driven invasion (Figure 2C). Consistent with this finding, overexpression of HIF-2 $\alpha$  in MCF-7 showed significantly enhanced invasion ability (Figure 2D).

Evidence suggested that hypoxia and EMT mutually promote each other under malignant conditions.<sup>31</sup> In this study, we found that morphologically, MCF-7/Flag maintained well-organized cell-cell contacts and cell polarity, while MCF-7/Flag-HIF cells revealed a spindle-like fibroblastic morphology, indicating characteristic morphological changes of EMT (Figure 2E). Meanwhile, the shape of MDA-MB-231 cells transfected with HIF2A-siRNA looked more like those of epithelial cells compared with controls (Figure 2E). These data suggested a vital involvement of HIF-2 $\alpha$  in EMT as well.

Together, these observations supported the roles for HIF-2 $\alpha$  in ATP pro-invasion and pro-EMT in vitro. Therefore, HIF-2 $\alpha$  was chosen for further investigation.

### 3.3 | Identification of hypoxia-inducible factor-2 $\alpha$ targets involved in ATP-promoted invasion and epithelial-mesenchymal transition

To investigate the downstream molecules involved in ATP-HIF-2 $\alpha$ -driven invasion, first, we focused on invasive-associated proteins. Matsumoto et al<sup>32</sup> demonstrated that stromal HIF-2 $\alpha$  induced LOX and MMP to promote trophoblast invasion using HIF-2 $\alpha$ -KO mice. Among LOX and MMP families, LOXL2<sup>33,34</sup> and MMP-9<sup>35</sup> were reported to be regulated via HIF under hypoxia status. In this study,

**FIGURE 2** Extracellular ATP promotes breast cancer cell invasion via hypoxia-inducible factor (HIF)-2 $\alpha$  in vitro. A, HIF-1/2 $\alpha$  expression was examined by western blotting. B, Western blotting demonstrated that HIF-1/2 $\alpha$  was decreased by digoxin (left). Transwell invasion assays illustrated that ATP-driven invasion was attenuated (right). C, Western blotting demonstrated that HIF-1/2 $\alpha$  was knocked down (left). Transwell invasion and migration assays showed that ATP-driven invasion and migration were attenuated via HIF2A-siRNA (right). D, Western blotting illustrated HIF-1/2 $\alpha$  elevation in stably transfected MCF-7 cells (left). Transwell invasion and migration assays showed that HIF-1/2 $\alpha$  enhanced MCF-7 invasion and migration capacities. E, The morphology of MCF-7/Flag-HIF-2 $\alpha$  cells looked like dispersed spindle-shaped mesenchymal cells, while MCF-7/Flag cells displayed cobblestone-like clusters of epithelial cells (upper). The shape of the MB-231/HIF2A-siRNA-treated cells looked more like the shape of epithelial cells (lower). Error bars represent means  $\pm$  SD from triplicate experiments. \* $P < 0.05$ ; \*\* $P < 0.01$ ; \*\*\* $P < 0.001$ ; ns, not significant

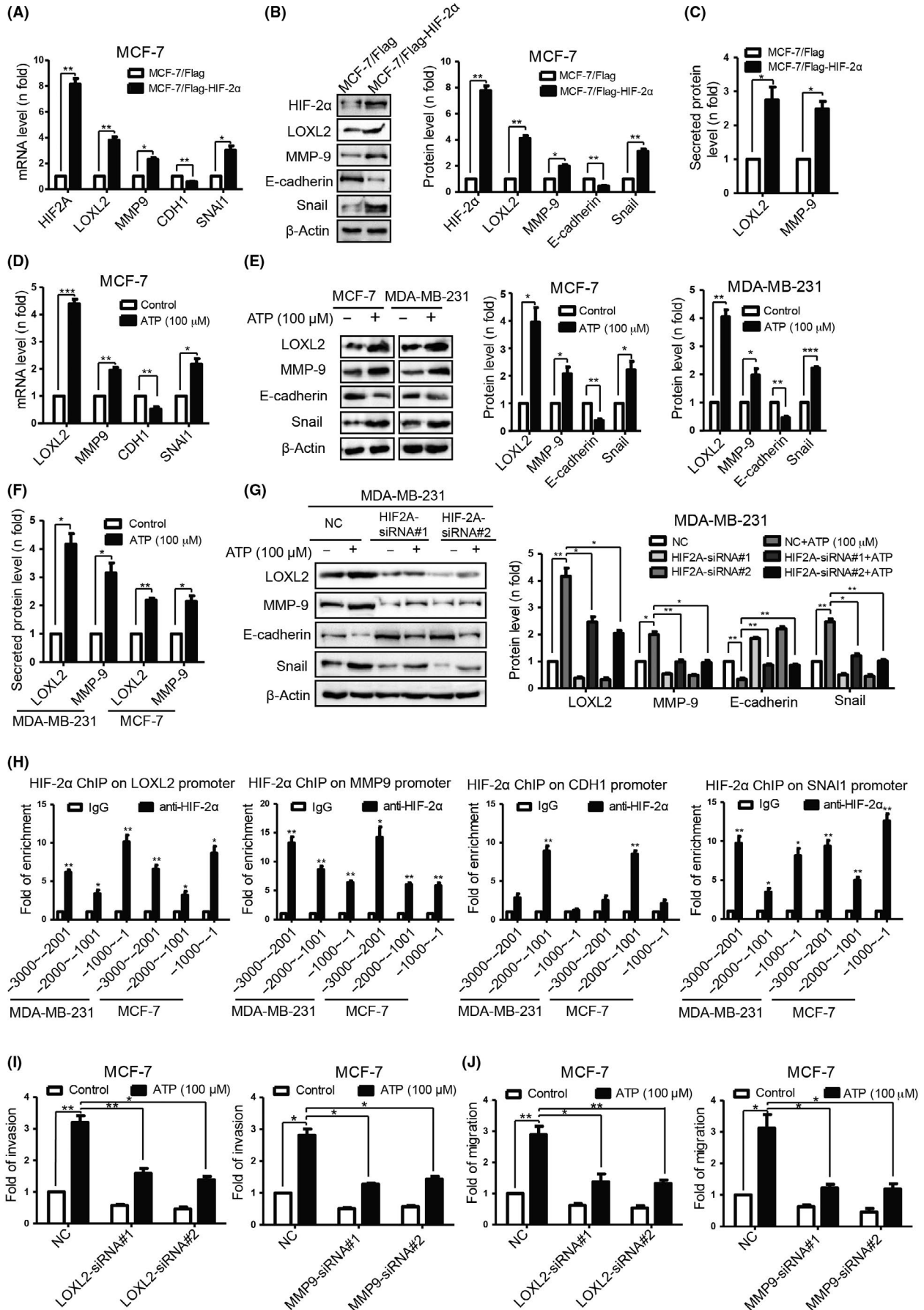


**FIGURE 3** ATP promotes invasion and epithelial-mesenchymal transition (EMT) via hypoxia-inducible factor (HIF) signaling-2 $\alpha$  targets LOXL2, MMP-9, E-cadherin and Snail, respectively. A, Quantitative PCR. B, western blotting demonstrated that expressions of indicated molecules were altered in MCF-7/Flag-HIF-2 $\alpha$  cells. C, ELISA proved that secreted LOXL2 and MMP-9 were elevated in MCF-7/Flag-HIF-2 $\alpha$  cells. D, Quantitative PCR. E, Western blotting. F, ELISA demonstrated alterations of indicated molecules in ATP-treated cells (24 h). G, Western blotting illustrated that ATP-driven alterations of indicated molecules were attenuated by HIF2 $\alpha$ -siRNA. H, qChIP analysis of the promoter of indicated molecules with antibodies against HIF-2 $\alpha$  proved that they were HIF-2 $\alpha$  direct target genes. I, Transwell invasion. J, Transwell migration assays showed that ATP-driven invasion and migration were attenuated by LOXL2- or MMP9-siRNA. Error bars represent means  $\pm$  SD from triplicates. \* $P$  < 0.05; \*\* $P$  < 0.01; \*\*\* $P$  < 0.001

we found that LOXL2 and MMP-9 could, indeed, be upregulated via HIF-2 $\alpha$  overexpression (Figure 3A-C) as well as ATP treatment (Figure 3D-F). Therefore, LOXL2 and MMP-9 were chosen for further study. Furthermore, knocking down HIF-2 $\alpha$  attenuated ATP-induced elevation of LOXL2 and MMP-9 (Figure 3G). In addition, qChIP assay using antibody against HIF-2 $\alpha$  demonstrated that LOXL2 and MMP9 were HIF-2 $\alpha$  direct target genes (Figure 3H). For functional experiments, both LOXL2-siRNA and MMP9-siRNA could attenuate ATP-driven invasion and migration (Figure 3I-J).

Hypoxia-inducible factor targets have been implicated in EMT, an early event in cancer metastasis.<sup>36</sup> To investigate the potential role of HIF-2 $\alpha$  in regulating EMT, we focused on epithelial marker E-cadherin and mesenchymal marker Snail, which were reported to be regulated via extracellular ATP in our previous research.<sup>16</sup> We found that E-cadherin and Snail levels could be regulated by

both HIF-2 $\alpha$  overexpression (Figure 3A,B) and ATP treatment (Figure 3D,E). Hence, E-cadherin and Snail were chosen for further study. Furthermore, knocking down HIF-2 $\alpha$  attenuated ATP-induced expression changes of E-cadherin and Snail (Figure 3G). By using the qChIP assay with antibody against HIF-2 $\alpha$ , we demonstrated that CDH1 and SNAI1 were HIF-2 $\alpha$  direct target genes (Figure 3H).

Collectively, these observations support the roles of HIF-2 $\alpha$  targets in ATP-driven invasion and EMT.

### 3.4 | Phosphoglycerate kinase 1 interacts with hypoxia-inducible factor-2 $\alpha$ and increases its expression

To investigate the functional mechanism of HIF-2 $\alpha$  in ATP-driven invasion, we used mass spectrometry to screen the proteins that are

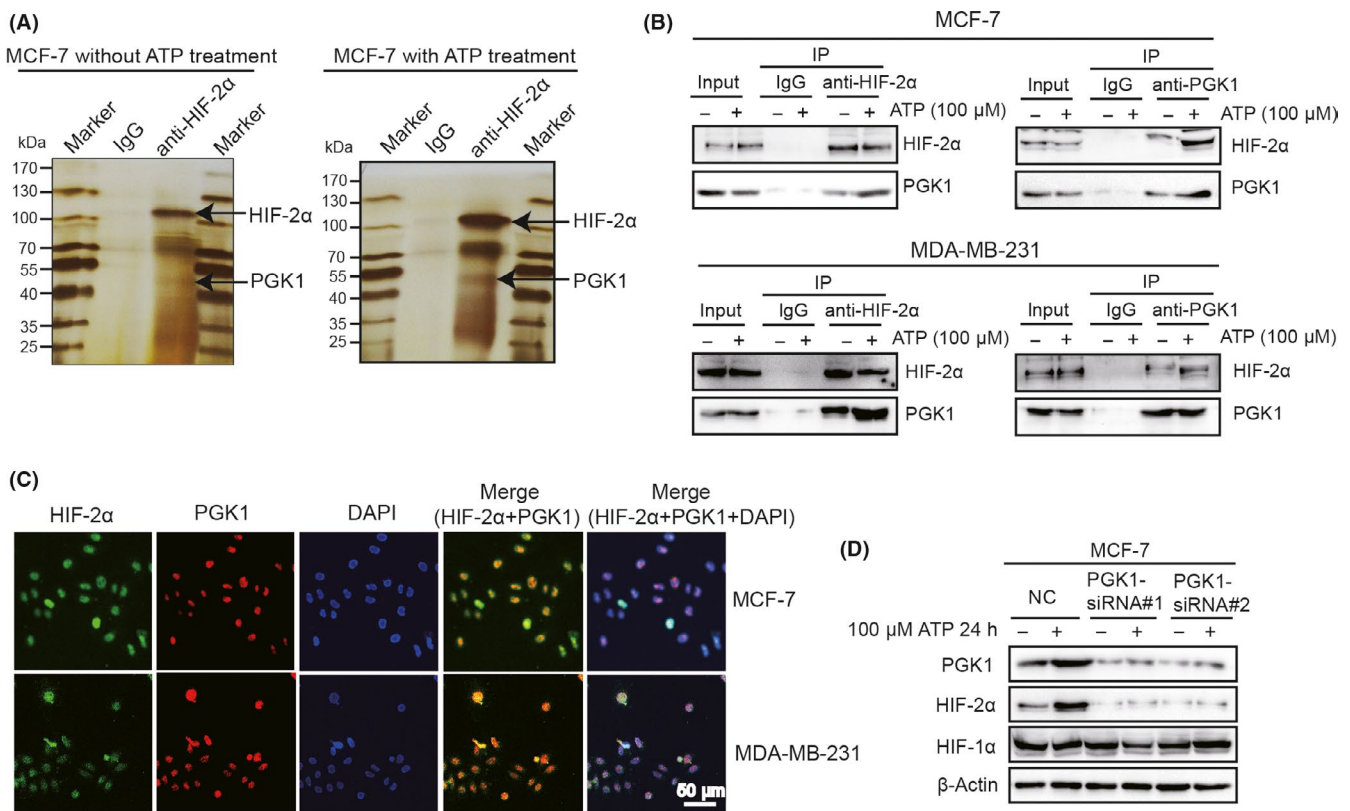


**FIGURE 4** Phosphoglycerate kinase 1 (PGK1) interacts with hypoxia-inducible factor (HIF)-2 $\alpha$  and mediates ATP-induced HIF-2 $\alpha$  elevation. A, MCF-7 cells were treated with/without ATP for 24 h. Cells were lysed and co-immunoprecipitated with anti-immunoglobulin G (IgG) or anti-HIF-2 $\alpha$ . The elutes were resolved by SDS-PAGE, silver-stained. The presence of PGK1 was detected by mass spectrometry. B, Physical interaction between PGK1 and HIF-2 $\alpha$  was determined by co-immunoprecipitation and western blotting. C, Cells were double-stained with HIF-2 $\alpha$  (green) and PGK1 (red) and counterstained with DAPI (blue). The merged regions indicated their co-localization. D, Western blotting demonstrated that PGK1-siRNA abolished ATP-driven upregulation of HIF-2 $\alpha$  but did not affect HIF-1 $\alpha$  expression



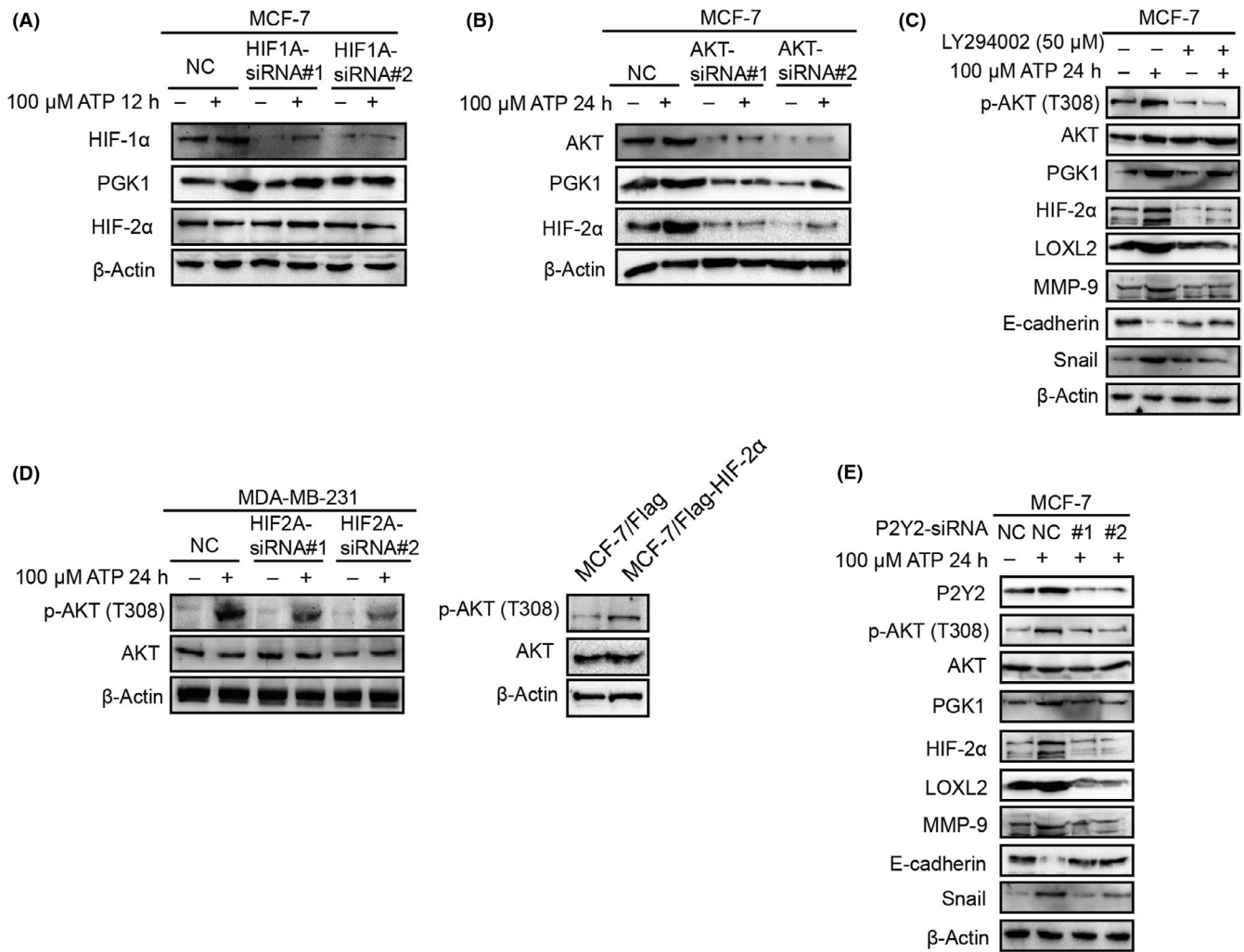


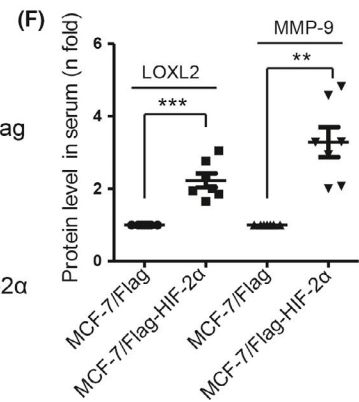
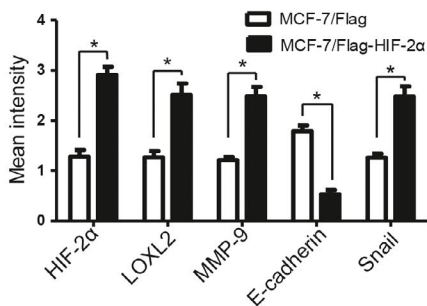
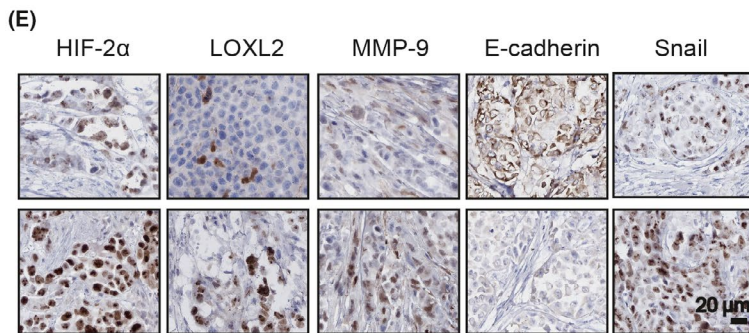
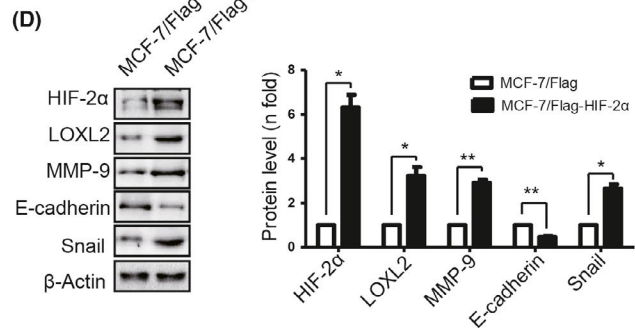
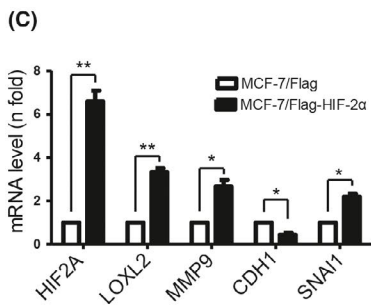
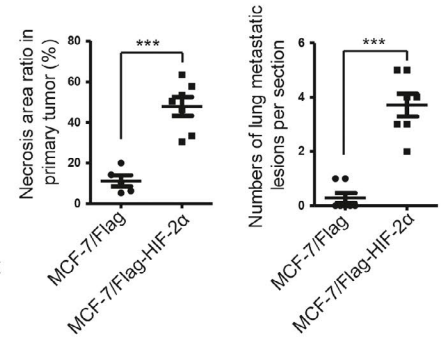
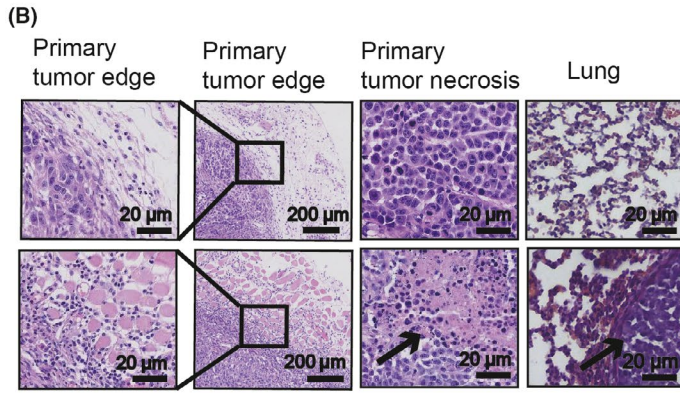
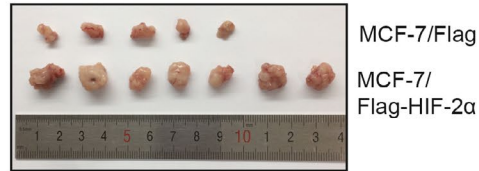
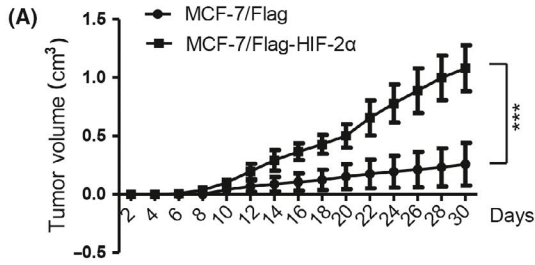
**FIGURE 5** ATP stimulates hypoxia-inducible factor (HIF)-2 $\alpha$  signaling via AKT pathway. A, Western blotting illustrated that HIF1A-siRNA did not affect phosphoglycerate kinase 1 (PGK1) or HIF-2 $\alpha$  expression. B, Western blotting demonstrated that ATP-induced elevation of HIF-2 $\alpha$  was abolished by AKT-siRNA. C, Western blotting demonstrated that ATP-induced expression changes of HIF-2 $\alpha$  and target proteins were attenuated by LY294002 (AKT inhibitor). D, Western blotting illustrated that phosphorylation of AKT could be regulated by HIF2A-siRNA (left) or Flag-HIF-2 $\alpha$  (right). E, Western blotting proved that P2Y2-siRNA attenuated ATP-mediated alterations in HIF-2 $\alpha$  signaling

interacted with HIF-2 $\alpha$  in vivo. Cellular extracts from MCF-7 with/without ATP treatment were co-immunoprecipitated by immunoglobulin G (IgG) or anti-HIF-2 $\alpha$  antibody, resolved on SDS-PAGE and visualized via silver staining (Figure 4A). The protein bands on the gel were recovered and then analyzed by mass spectrometry. The results indicated that HIF-2 $\alpha$  co-immunoprecipitated with proteins, including PGK1 (Appendix S5), ALDOC, and ENO2, etc. Evidence suggested that PGK1, which was considered as a vital kinase in cellular activity<sup>37</sup> and a target gene of HIF-1 $\alpha$ ,<sup>37</sup> could form a positive feed-forward loop with HIF-1 $\alpha$  and, thus, stimulated breast cancer

progression and metastases.<sup>38</sup> However, we discovered that PGK1 could form a complex with HIF-2 $\alpha$  using silver staining and mass spectrometry, which seemed interesting. To confirm this result, we checked for physical interaction between PGK1 and HIF-2 $\alpha$  following ATP treatment by co-immunoprecipitation in MCF-7 and MDA-MB-231 (Figure 4B). Moreover, we observed co-localization of HIF-2 $\alpha$  and PGK1 via immunofluorescence (Figure 4C), which further suggests their interaction.

Because PGK1 could interact with HIF-2 $\alpha$ , we wondered whether PGK1 could affect HIF-2 $\alpha$  expression. We found that ATP

**FIGURE 6** Hypoxia-inducible factor (HIF)-2 $\alpha$  promotes xenograft tumor growth and metastasis in vivo. A, MCF-7/Flag or MCF-7/Flag-HIF-2 $\alpha$  cells were inoculated orthotopically onto the mammary fat pad of 6-wk-old female Balb/c mice (n = 7). Tumor volumes were quantified every 2 days (left) and tumors were shown on the 30th day (right). B, Primary tumor and representative metastasis specimens were H&E stained (left). Necrosis area ratio in primary tumors and numbers of metastatic lesions in lungs were quantified (right). C-E, Expressions of HIF-2 $\alpha$  and its targets were examined by quantitative PCR (C), western blotting (D) and immunohistochemistry (IHC) staining (E) from primary tumor tissue of each mouse. F, LOXL2 and MMP-9 levels were detected by ELISA. Error bars represent means  $\pm$  SD from triplicates. \* $P < 0.05$ ; \*\* $P < 0.01$ ; \*\*\* $P < 0.001$



upregulated PGK1 expression as well (Figures 1C,4D) and PGK1-siRNA attenuated ATP-driven HIF-2 $\alpha$  elevation but did not affect HIF-1 $\alpha$  expression (Figure 4D), suggesting that PGK1 specifically mediates ATP-induced HIF-2 $\alpha$  elevation.

### 3.5 | Extracellular ATP stimulates phosphoglycerate kinase 1-hypoxia-inducible factor-2 $\alpha$ signaling via AKT pathway

To investigate the regulation of PGK1-HIF-2 $\alpha$  via extracellular ATP, first, we focused on HIF-1 $\alpha$ , of which PGK1 was generally identified as a target gene.<sup>37</sup> Regrettably, knocking down HIF-1 $\alpha$  did not influence ATP-induced PGK1 upregulation, suggesting that HIF-1 $\alpha$  was not involved in this signaling (Figure 5A). Evidence suggested that AKT signaling, which can be stimulated via ATP, as demonstrated in our previous study,<sup>14</sup> activated PGK1 by decreasing K220 acetylation of endogenous PGK1.<sup>39</sup> Therefore, we speculated that AKT might be involved in PGK1-HIF-2 $\alpha$  signaling in ATP treatment. As a result, blocking AKT signaling using AKT-siRNA or LY294002 (AKT inhibitor) significantly attenuated expressions of PGK1 and HIF-2 $\alpha$  (Figure 5B,C), as well as HIF-2 $\alpha$  target proteins (Figure 5C).

Interestingly, knocking down HIF-2 $\alpha$  in MDA-MB-231 cells abolished ATP-induced phosphorylation of AKT. Meanwhile, overexpression of HIF-2 $\alpha$  in MCF-7 indeed increased the AKT phosphorylation level, suggesting that there might be a reciprocal feedback loop between ATP-driven HIF-2 $\alpha$  and AKT signaling (Figure 5D).

We had demonstrated that P2Y2 receptor mediated ATP-driven invasion and AKT signaling activation in cancer cells.<sup>12,13,15,16</sup> Here, we found that P2Y2-siRNA also abolished AKT-PGK1-HIF-2 $\alpha$  signaling in ATP treatment (Figure 5E).

Taken together, these results suggest that it is the AKT pathway that modulates PGK1-HIF-2 $\alpha$  signaling in ATP treatment.

### 3.6 | Hypoxia-inducible factor-2 $\alpha$ promotes xenograft tumor growth and metastasis in vivo

To explore the role of HIF-2 $\alpha$  in breast cancer metastasis in vivo, a Balb/c mice model was used. Five million MCF-7/Flag-HIF-2 $\alpha$  and MCF-7/Flag control cells were orthotopically implanted into the mammary fat pad of 6-week-old female mice (7 for each group). The growth of primary tumors was monitored every 2 days over a period of 1 month. As a result, the MCF-7/Flag-HIF-2 $\alpha$  injected group exhibited increased tumor growth (Figure 6A), necrosis and lung metastasis (Figure 6B). In addition, tumors in the MCF-7/Flag-HIF-2 $\alpha$ -injected group demonstrated apparent invasion into the neighboring tissues (Figure 6B).

Then, using quantitative RT-PCR (Figure 6C), western blotting (Figure 6D) and IHC staining (Figure 6E), we examined expression changes of HIF-2 $\alpha$  and its targets, which were in line with our previous findings in vitro. In addition, peripheral LOXL2 and MMP-9 levels in the MCF-7/Flag-HIF-2 $\alpha$  group were significantly increased (Figure 6F).

Taken together, HIF-2 $\alpha$  promoted xenograft tumor growth and metastasis in mice, which further confirmed our in vitro ATP-HIF-2 $\alpha$  signaling.

### 3.7 | The ATP-hypoxia-inducible factor-2 $\alpha$ axis is associated with clinical breast cancer progression

To further investigate the role of the ATP-HIF-2 $\alpha$  signaling in human cancers and to explore the clinical significance, we analyzed ATP-HIF-2 $\alpha$  signaling-associated genes using the Oncomine database (<https://www.oncomine.org/>) (Figure 7A). The expressions of HIF2A, AKT, LOXL2, MMP9, SNAI1 and PGK1 were relatively higher in breast cancer tissues than in normal breast tissues. Moreover, Kaplan-Meier survival analysis (<http://kmpplot.com/analysis/>) showed that high levels of PGK1, LOXL2, MMP9 and SNAI1 were associated with worse survival rates in breast cancer patients (Figure 7B). Altogether, these data were consistent with our previous discoveries.

## 4 | DISCUSSION

It has been demonstrated that during cancer growth and invasion, ATP is highly enriched in the tumor extracellular environment and fulfills a key role as an extracellular messenger.<sup>7,40</sup> As early as 2008, it was demonstrated that ATP levels in the extracellular milieu of solid tumors could reach hundreds of micromoles, which is much higher than the usual concentration of this nucleotide in the interstitium of healthy tissues (10-100 nmol/L).<sup>41</sup> Hence, the 100  $\mu$ mol/L extracellular ATP treatment used in our research is a suitable simulation of the in vivo tumor microenvironment.

Based on cDNA microarray data and KEGG pathway analysis, extracellular ATP activated quite a few signalings. The reasons that HIF or HIF-2 $\alpha$  was chosen for further investigation were as follows: (i) HIF-1/2 $\alpha$  is a vital transcription factor in tumor progression;<sup>42</sup> (ii) although the elevation of HIF-1/2 $\alpha$  in hypoxia status has been well investigated, the exact molecular mechanisms underlying HIF activity in normoxic have not been fully elucidated, and we are the first to demonstrate that ATP could upregulate HIF-1/2 $\alpha$  expression under normoxic and determined that it was HIF-2 $\alpha$  that played a dominant role in ATP-driven invasion and the EMT process; and (iii) the Oncomine database showed that HIF2A was highly expressed in breast cancer tissues (Figure 7A), and HPA, GTEX and FANTOM5 datasets showed that HIF2A was expressed in all cancer categories (<https://www.proteinatlas.org/>). Therefore, HIF-2 $\alpha$  could serve as a possible molecular target in tumor therapies.

Multiple genetic alterations confer hyperactivation of AKT in human solid tumors and hematological malignancies.<sup>43</sup> Our previous research revealed the involvement of AKT signaling in bFGF-driven HIF-1 $\alpha$  activation.<sup>20</sup> In this study, we demonstrated that extracellular ATP activated AKT-PGK1-HIF-2 $\alpha$  signaling in breast cancer cells. The possible explanation might be that HIF-1 $\alpha$  and HIF-2 $\alpha$  have 48% amino acid identity and similar protein structures, and might display both unique and overlapping patterns in molecular signaling pathways.<sup>44</sup> Although PGK1 was generally identified as a direct target of HIF-1 $\alpha$ ,<sup>37</sup> here we demonstrated that it was AKT, not HIF-1 $\alpha$ , that functioned upstream of PGK1-HIF-2 $\alpha$  in ATP treatment.

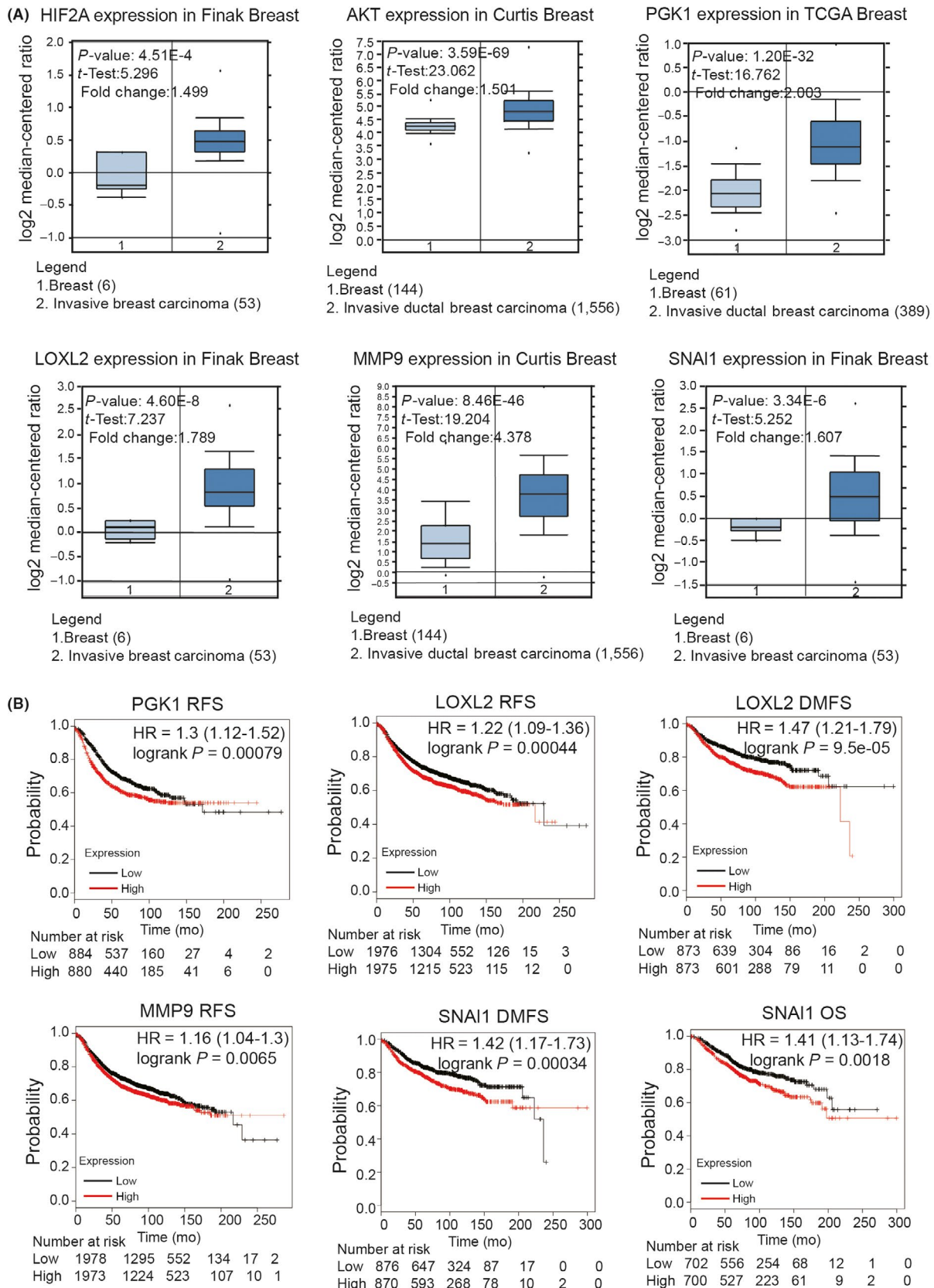


**FIGURE 7** ATP-hypoxia-inducible factor (HIF)-2 $\alpha$ -axis is associated with clinical breast cancer progression. A, Analysis of Oncomine dataset illustrated significant difference of ATP-HIF-2 $\alpha$  signaling-related genes between breast carcinoma and normal mammary tissues. B, Kaplan-Meier survival analysis showed the negative correlations between survival time of breast cancer patients and levels of PGK1, LOXL2, MMP9 and SNAI1. DMFS, distant metastasis-free survival; OS, overall survival; RFS, relapse-free survival

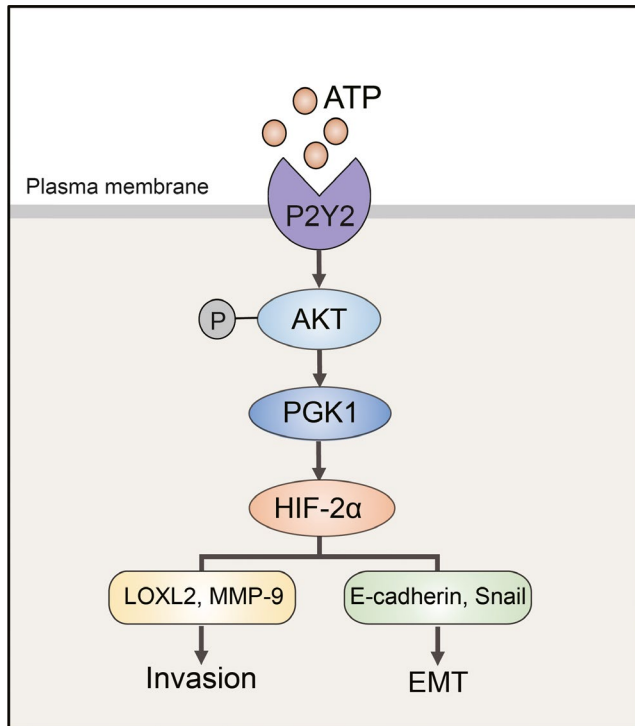


**FIGURE 8** The proposed model for the ATP-hypoxia-inducible factor (HIF) signaling-2 $\alpha$  axis in breast cancer invasion and the epithelial-mesenchymal transition (EMT) process. ATP could upregulate HIF-2 $\alpha$  via AKT-PGK1 signaling, provoking HIF-2 $\alpha$  targets, among which LOXL2 and MMP-9 mediate ATP-driven invasion, and E-cadherin and Snail mediate ATP-driven EMT

The P2Y2 receptor was demonstrated to play a vital role in ATP-HIF-2 $\alpha$  signaling in this study. The detailed reasons for examining the involvement of P2Y2 were: (i) compared with MCF-10A, breast cancer cells showed higher P2Y2 levels;<sup>15</sup> (ii) the TCGA database showed that P2Y2 was highly expressed in breast cancer tissues as well;<sup>15</sup> and (iii) ATP is the preferred ligand for P2Y2 receptor and our previous studies had demonstrated that P2Y2 played an important role in ATP-mediated invasion and AKT activation.<sup>12,13,15,16</sup> However, considering that ATP could function via quite a few receptors, whether there was other receptor involved in this process needs to be explored further in the future.

Epithelial-mesenchymal transition is a vital step during cancer progression.<sup>14</sup> In this research, we identified HIF-2 $\alpha$  mediated ATP pro-EMT function via E-cadherin and Snail, which are well-known EMT markers.<sup>45,46</sup> We noticed that HIF-2 $\alpha$  directly bound to the CDH1 promoter and suppressed its expression. The function of a transcription factor might depend on cell type specificity,<sup>47</sup> tissue type specificity or partner proteins.<sup>48</sup> For example, if one transcription factor interacts with corepressor complexes, it is possible to repress target gene expressions.<sup>28</sup> Besides PGK1, we speculated that HIF-2 $\alpha$  also had other partner proteins, because silver staining showed that bands existed in that anti-HIF-2 $\alpha$  group (Figure 4A). Hence, it is possible that corepressor complexes functioned in this process. It is worth mentioning that the O<sub>2</sub> level could also determine partner proteins and targets of HIF.<sup>49</sup>

Therefore, the regulation of target genes of HIF could even vary under different O<sub>2</sub> levels.

In fact, subsequent metastatic spread is a complex process resulting from the coordinated and sequential events of cancer cells.<sup>3</sup> Among those, degradation and reorganization of the extracellular matrix (ECM), which is generally facilitated by the release of MMP<sup>50</sup> and LOX,<sup>51</sup> is considered a vital step.<sup>3</sup> Salvador et al<sup>52</sup> reported that LOXL2 was involved in the metastatic process via modifying the ECM stiffness in PyMT tumors. Evidence highlights a dominant role for MMP-9 in breast cancer invasion as well.<sup>53</sup> These results were in line with our findings that LOXL2 and MMP-9 functioned as HIF-2 $\alpha$  targets and could mediate the ATP-driven invasion process.

The limitations of our research included that, first, we focused on HIF-2 $\alpha$ -mediated invasion and the EMT process without specifically concentrating on ATP-HIF-2 $\alpha$ -mediated cellular functions. However, even though it is a well-known phenomenon, the novelty of our research elaborates on a new mechanism of ATP-HIF-2 $\alpha$  under normoxia conditions. Second, we only demonstrated that an interaction existed between PGK1 and HIF-2 $\alpha$  without identifying the interacting domains. We will attempt to identify the interaction domains of PGK1 and HIF-2 $\alpha$  in the future.

Taken together, we are the first to illustrate that HIF-2 $\alpha$  could be elevated via extracellular ATP under normoxic conditions. We revealed the roles of ATP-HIF-2 $\alpha$  in promoting breast cancer invasion and EMT. As direct targets of HIF-2 $\alpha$ , LOXL2 and MMP-9 mediate ATP-driven invasion, and E-cadherin and Snail mediate ATP-induced EMT. Both HIF-2 $\alpha$  and its targets could be regulated via AKT-PGK1 signaling by ATP (Figure 8). These findings have significant implications regarding our understanding of breast cancer progression. The pleiotropic effects of ATP-HIF-2 $\alpha$  signaling in invasion and EMT suggest that it could be an effective target for breast cancer therapy.

## ACKNOWLEDGMENTS

This work was supported by grants to Xin-Xia Tian and Wei-Gang Fang from the National Natural Science Foundation of China (Nos. 81872382 and 81621063).

## DISCLOSURE

The authors declare no competing interests.

## ORCID

Hong-Quan Zhang  <https://orcid.org/0000-0001-8193-0899>

Xin-Xia Tian  <https://orcid.org/0000-0002-1593-4987>

## REFERENCES

1. Liu Y, Geng YH, Yang H, et al. Extracellular ATP drives breast cancer cell migration and metastasis via S100A4 production by cancer cells and fibroblasts. *Cancer Lett*. 2018;430:1-10.

2. Verrax J, Dejeans N, Sid B, Glorieux C, Calderon PB. Intracellular ATP levels determine cell death fate of cancer cells exposed to both standard and redox chemotherapeutic agents. *Biochem Pharmacol*. 2011;82:1540-1548.
3. Di Virgilio F, Sarti AC, Falzoni S, De Marchi E, Adinolfi E. Extracellular ATP and P2 purinergic signalling in the tumour microenvironment. *Nat Rev Cancer*. 2018;18:601-618.
4. Zhao S, Torres A, Henry RA, et al. ATP-citrate lyase controls a glucose-to-acetate metabolic switch. *Cell Rep*. 2016;17:1037-1052.
5. Techatharati O, Nowwarote N, Taebunpakul S, Pavasant P. Biphasic effect of ATP on in vitro mineralization of dental pulp cells. *J Cell Biochem*. 2018;119:488-498.
6. Forrester T. A case of serendipity\*. *Purinergic Signal*. 2008;4:93-100.
7. Burnstock G. Physiology and pathophysiology of purinergic neurotransmission. *Physiol Rev*. 2007;87:659-797.
8. Morciano G, Sarti AC, Marchi S, et al. Use of luciferase probes to measure ATP in living cells and animals. *Nat Protoc*. 2017;12:1542-1562.
9. Vijayan D, Young A, Teng MWL, Smyth MJ. Targeting immunosuppressive adenosine in cancer. *Nat Rev Cancer*. 2017;17:765.
10. Di Virgilio F, Adinolfi E. Extracellular purines, purinergic receptors and tumor growth. *Oncogene*. 2017;36:293-303.
11. Fang WG, Pirnia F, Bang YJ, Myers CE, Trepel JB. P2-purinergic receptor agonists inhibit the growth of androgen-independent prostate carcinoma cells. *J Clin Invest*. 1992;89:191-196.
12. Li WH, Qiu Y, Zhang HQ, et al. P2Y2 receptor promotes cell invasion and metastasis in prostate cancer cells. *Br J Cancer*. 2013;109:1666-1675.
13. Li WH, Qiu Y, Zhang HQ, Tian XX, Fang WG. P2Y2 receptor and EGFR cooperate to promote prostate cancer cell invasion via ERK1/2 pathway. *PLoS ONE*. 2015;10:e0133165.
14. Qiu Y, Li WH, Zhang HQ, Liu Y, Tian XX, Fang WG. P2X7 mediates ATP-driven invasiveness in prostate cancer cells. *PLoS ONE*. 2014;9:e114371.
15. Zhang JL, Liu Y, Yang H, Zhang HQ, Tian XX, Fang WG. ATP-P2Y2-beta-catenin axis promotes cell invasion in breast cancer cells. *Cancer Sci*. 2017;108:1318-1327.
16. Qiu Y, Liu Y, Li WH, Zhang HQ, Tian XX, Fang WG. P2Y2 receptor promotes the migration and invasion of breast cancer cells via EMT-related genes snail and E-cadherin. *Oncol Rep*. 2018;39:138-150.
17. Yamamura K, Uruno T, Shiraishi A, et al. The transcription factor EPAS1 links DOCK8 deficiency to atopic skin inflammation via IL-31 induction. *Nat Commun*. 2017;8:13946.
18. Wu D, Potluri N, Lu J, Kim Y, Rastinejad F. Structural integration in hypoxia-inducible factors. *Nature*. 2015;524:303-308.
19. Koh MY, Spivak-Kroizman TR, Powis G. HIF-1 $\alpha$  and cancer therapy. *Recent Results Cancer Res*. 2010;180:15-34.
20. Shi YH, Wang YX, Bingle L, et al. In vitro study of HIF-1 activation and VEGF release by bFGF in the T47D breast cancer cell line under normoxic conditions: involvement of PI-3K/Akt and MEK1/ERK pathways. *J Pathol*. 2005;205:530-536.
21. Holmquist-Mengelbier L, Fredlund E, Lofstedt T, et al. Recruitment of HIF-1 $\alpha$  and HIF-2 $\alpha$  to common target genes is differentially regulated in neuroblastoma: HIF-2 $\alpha$  promotes an aggressive phenotype. *Cancer Cell*. 2006;10:413-423.
22. Raval RR, Lau KW, Tran MG, et al. Contrasting properties of hypoxia-inducible factor 1 (HIF-1) and HIF-2 in von Hippel-Lindau-associated renal cell carcinoma. *Mol Cell Biol*. 2005;25:5675-5686.
23. Cho H, Du X, Rizzi JP, et al. On-target efficacy of a HIF-2 $\alpha$  antagonist in preclinical kidney cancer models. *Nature*. 2016;539:107-111.
24. Uchida T, Rossignol F, Matthay MA, et al. Prolonged hypoxia differentially regulates hypoxia-inducible factor (HIF)-1 $\alpha$  and HIF-2 $\alpha$  expression in lung epithelial cells: implication of natural antisense HIF-1 $\alpha$ . *J Biol Chem*. 2004;279:14871-14878.
25. Franovic A, Holterman CE, Payette J, Lee S. Human cancers converge at the HIF-2 $\alpha$  oncogenic axis. *Proc Natl Acad Sci USA*. 2009;106:21306-21311.
26. Scrideli CA, Carlotti CG Jr, Mata JF, et al. Prognostic significance of co-overexpression of the EGFR/IGFBP-2/HIF-2A genes in astrocytomas. *J Neurooncol*. 2007;83:233-239.
27. Yuan JH, Yang F, Wang F, et al. A long noncoding RNA activated by TGF-beta promotes the invasion-metastasis cascade in hepatocellular carcinoma. *Cancer Cell*. 2014;25:666-681.
28. Shan L, Zhou X, Liu X, et al. FOXK2 elicits massive transcription repression and suppresses the hypoxic response and breast cancer carcinogenesis. *Cancer Cell*. 2016;30:708-722.
29. Koh MY, Lemos R Jr, Liu X, Powis G. The hypoxia-associated factor switches cells from HIF-1 $\alpha$ - to HIF-2 $\alpha$ -dependent signaling promoting stem cell characteristics, aggressive tumor growth and invasion. *Cancer Res*. 2011;71:4015-4027.
30. Zhang H, Qian DZ, Tan YS, et al. Digoxin and other cardiac glycosides inhibit HIF-1 $\alpha$  synthesis and block tumor growth. *Proc Natl Acad Sci USA*. 2008;105:19579-19586.
31. Liu K, Sun B, Zhao X, et al. Hypoxia induced epithelial-mesenchymal transition and vasculogenic mimicry formation by promoting Bcl-2/Twist1 cooperation. *Exp Mol Pathol*. 2015;99:383-391.
32. Matsumoto L, Hirota Y, Saito-Fujita T, et al. HIF2 $\alpha$  in the uterine stroma permits embryo invasion and luminal epithelium detachment. *J Clin Invest*. 2018;128:3186-3197.
33. Higgins DF, Kimura K, Bernhardt WM, et al. Hypoxia promotes fibrogenesis in vivo via HIF-1 stimulation of epithelial-to-mesenchymal transition. *J Clin Invest*. 2007;117:3810-3820.
34. Schietke R, Warnecke C, Wacker I, et al. The lysyl oxidases LOX and LOXL2 are necessary and sufficient to repress E-cadherin in hypoxia: insights into cellular transformation processes mediated by HIF-1. *J Biol Chem*. 2010;285:6658-6669.
35. Choi JY, Jang YS, Min SY, Song JY. Overexpression of MMP-9 and HIF-1 $\alpha$  in breast cancer cells under hypoxic conditions. *J Breast Cancer*. 2011;14:88-95.
36. Yang MH, Wu MZ, Chiou SH, et al. Direct regulation of TWIST by HIF-1 $\alpha$  promotes metastasis. *Nat Cell Biol*. 2008;10:295-305.
37. Li X, Jiang Y, Meisenhelder J, et al. Mitochondria-translocated PGK1 functions as a protein kinase to coordinate glycolysis and the TCA cycle in tumorigenesis. *Mol Cell*. 2016;61:705-719.
38. Fu D, He C, Wei J, et al. PGK1 is a potential survival biomarker and invasion promoter by regulating the HIF-1 $\alpha$ -mediated epithelial-mesenchymal transition process in breast cancer. *Cell Physiol Biochem*. 2018;51:2434-2444.
39. Wang S, Jiang B, Zhang T, et al. Correction: insulin and mTOR pathway regulate HDAC3-mediated deacetylation and activation of PGK1. *PLoS Biol*. 2015;13:e1002287.
40. Burnstock G, Di Virgilio F. Purinergic signalling and cancer. *Purinergic Signal*. 2013;9:491-540.
41. Pellegatti P, Raffaghello L, Bianchi G, Piccardi F, Pistoia V, Di Virgilio F. Increased level of extracellular ATP at tumor sites: in vivo imaging with plasma membrane luciferase. *PLoS ONE*. 2008;3:e2599.
42. Monteiro AR, Hill R, Pilkington GJ, Madureira PA. The role of hypoxia in glioblastoma invasion. *Cells*. 2017;6.
43. Manning BD, Toker A. AKT/PKB signaling: navigating the network. *Cell*. 2017;169:381-405.
44. Hu CJ, Wang LY, Chodosh LA, Keith B, Simon MC. Differential roles of hypoxia-inducible factor 1 alpha (HIF-1 $\alpha$ ) and HIF-2 $\alpha$  in hypoxic gene regulation. *Mol Cell Biol*. 2003;23:9361-9374.
45. Thiery JP. Epithelial-mesenchymal transitions in tumour progression. *Nat Rev Cancer*. 2002;2:442-454.
46. Nieto MA, Huang RY, Jackson RA, Thiery JP. EMT: 2016. *Cell*. 2016;166:21-45.
47. Chi JT, Wang Z, Nuyten DS, et al. Gene expression programs in response to hypoxia: cell type specificity and prognostic significance in human cancers. *PLoS Med*. 2006;3:e47.

48. Pritchett J, Athwal V, Roberts N, Hanley NA, Hanley KP. Understanding the role of SOX9 in acquired diseases: lessons from development. *Trends Mol Med*. 2011;17:166-174.
49. Sadri N, Zhang PJ. Hypoxia-inducible factors: mediators of cancer progression; prognostic and therapeutic targets in soft tissue sarcomas. *Cancers (Basel)*. 2013;5:320-333.
50. Kurbet AS, Hegde S, Bhattacharjee O, Marepally S, Vemula PK, Raghavan S. Sterile inflammation enhances ECM degradation in integrin beta1 KO embryonic skin. *Cell Rep*. 2016;16:3334-3347.
51. Rossow L, Veitl S, Vorlova S, et al. LOX-catalyzed collagen stabilization is a proximal cause for intrinsic resistance to chemotherapy. *Oncogene*. 2018;37:4921-4940.
52. Salvador F, Martin A, Lopez-Menendez C, et al. Lysyl oxidase-like protein LOXL2 promotes lung metastasis of breast cancer. *Cancer Res*. 2017;77:5846-5859.
53. Bai XY, Li S, Wang M, et al. Kruppel-like factor 9 down-regulates matrix metalloproteinase 9 transcription and suppresses human breast cancer invasion. *Cancer Lett*. 2018;412:224-235.

## SUPPORTING INFORMATION

Additional supporting information may be found online in the Supporting Information section at the end of the article.

**How to cite this article:** Yang H, Geng Y-H, Wang P, et al. Extracellular ATP promotes breast cancer invasion and epithelial-mesenchymal transition via hypoxia-inducible factor 2 $\alpha$  signaling. *Cancer Sci*. 2019;110:2456-2470. <https://doi.org/10.1111/cas.14086>